Analytical Solution of the Optimal Steering Law for Non-Ideal Solar Sail

Lorenzo Niccolai, Alessandro A. Quarta*, Giovanni Mengali

Department of Civil and Industrial Engineering, University of Pisa, I-56122 Pisa, Italy

Abstract

This paper analyzes the problem of finding the optimal steering law for a flat solar sail whose propulsive acceleration is described by an optical force model. In particular, the problem amounts to looking for the optimal direction of the unit vector normal to the sail plane that maximizes the projection of the propulsive acceleration along a given direction. Starting from the known results from the literature, according to which a close form solution for the general case of not (fully) specularly reflecting sail cannot be retrieved, the propulsive acceleration is approximated by a mathematical model that closely resembles the classical optical force model. Using this new approach, the solution of the optimal steering law is shown to be written in an analytical form that is fully general and extremely accurate. In this sense, the proposed mathematical model may effectively be used to analyze the impact of the thermo-optical characteristics of the sail film on the optimal steering law within a wide range of different mission scenarios.

Keywords: Solar sail, Optical force model, Optimal control law

Nomenclature

A	=	function of θ and B, see Eq. (38)
A_s	=	sail area, $[\mathrm{m}^2]$
$\boldsymbol{a}$	=	propulsive acceleration, $[\mathrm{mm/s}^2]$
a_c	=	spacecraft characteristic acceleration, $[\mathrm{mm/s}^2]$
$a_\perp, a_\parallel$	=	components of the propulsive acceleration along $\hat{\boldsymbol{n}}$ and $\hat{\boldsymbol{t}}$, respectively, $[\mathrm{mm/s}^2]$
a_r, a_n	=	components of the propulsive acceleration along $\hat{\boldsymbol{r}}$ and $\hat{\boldsymbol{n}}$, respectively, $[\mathrm{mm/s}^2]$
B	=	reduced force coefficient
B_b, B_f	=	non-Lambertian coefficients of the back and front sail surface
b_1, b_2, b_3	=	solar sail force coefficients
D	=	function of θ and B, see Eq. (40)
f	=	auxiliary function
J	=	performance index
m	=	spacecraft mass, $[\mathrm{kg}]$
$\hat{\boldsymbol{n}}$	=	normal unit vector
$\mathcal{P}$	=	plane spanned by $\hat{\boldsymbol{r}}$ and $\hat{\boldsymbol{q}}$
$P_\oplus$	=	solar radiation pressure at $r = 1\,\mathrm{au}$, $[\mathrm{N/m}^2]$
Q	=	polynomial in x
$\hat{\boldsymbol{q}}$	=	fixed unit vector
$\boldsymbol{r}$	=	Sun-spacecraft vector, with $r = \|\boldsymbol{r}\|$, $[\mathrm{au}]$
$r_\oplus$	=	reference distance $(1\,\mathrm{au})$

*Corresponding author

Email addresses: lorenzo.niccolai@ing.unipi.it (Lorenzo Niccolai), a.quarta@ing.unipi.it (Alessandro A. Quarta), g.mengali@ing.unipi.it (Giovanni Mengali)

Published in Aerospace Science and Technology, online before print, December 2016. doi: http://dx.doi.org/10.1016/j.ast.2016.11.031

s = specular reflection fraction of sail film
$\hat{\boldsymbol{t}}$ = unit vector parallel to the sail plane
x = auxiliary variable
α = cone angle, [deg]
$\alpha^\star$ = optimal cone angle, [deg]
$\widetilde{\alpha}$ = cone angle corresponding to a local maximum of J, [deg]
ε = error parameter
ϵ = emissivity of sail film
η = reduction coefficient of the sail thrust in the η-perfect reflection model
θ = cone angle of $\hat{\boldsymbol{q}}$, [deg]
θ_i = function of B, with $i = 1, 2, 3, 4$
ρ = reflection coefficient of sail film
ϕ = function of θ and B, see Eq. (39)

Subscripts

a = approximated
max = maximum
min = minimum
b = back surface
f = front surface

Superscripts

$\wedge$ = unit vector

1. Introduction

The solar sail concept represents one of the most promising innovations within the field of low thrust propulsion systems, as is clearly demonstrated by the recent success of the Japanese mission IKAROS [1], when a small solar sail was first deployed and then actively controlled in interplanetary space [2, 3]. The renewed impulse received by the photonic-based space propulsion is also confirmed by two new planned NASA missions that are going to be equipped with a solar sail [4, 5].

For these reasons, it is extremely useful to have suitable mathematical tools to be used during the mission analysis of a solar sail-based spacecraft. In most cases the solar sail trajectory is analyzed within an optimal framework, by looking for the steering law that maximises a given scalar performance index, which usually coincides with the total flight time. The literature involving such a subject, starting from the pioneering work by Zhukov and Lebedev [6], offers several examples [7, 8, 9] in which the optimal steering law is studied as a function of the physical characteristics of the solar sail reflecting film, that is, of the so called sail force model.

The simplest sail force model, referred to as ideal model, consists in assuming the propulsive acceleration equivalent to that obtained from a flat and specularly reflecting solar sail [10]. The ideal model can be refined by taking into account the thermo-optical characteristics of the reflecting film, but retaining the fundamental assumption of flat solar sail. This corresponds to the optical force model. The sail billowing effect due to the solar radiation pressure is accounted for in the so called parametric force model [11], which relates the thrust vector direction with the sail attitude orientation through an interpolation of numerical-experimental data. However, the optical force model is the best compromise between accuracy and simplicity of the model. In fact, the parametric model is not much used in a preliminary mission analysis for several reasons: it is tailored on a specific sail configuration and requires specific experimental data, it is difficult to update during the mission when, for example, the sail degradation effects must be taken into account, and it is more complex to insert within an optimization algorithm.

The algorithms needed for calculating the optimal steering law in analytic form are extremely important, since they assure a significant reduction of the computational time for simulating the spacecraft optimal

trajectories, especially when the solar sail has medium or low performance. Even in the simplified case of a flat solar sail, that is, neglecting any billowing effect, a fully analytical solution of the optimal steering law is available only when the propulsive acceleration is assumed to be directed along the normal to the sail plane. This happens, for example, in the ideal case of fully specular reflection of the impinging photons [7], or in the case of imperfect reflectivity that simply reduces by a factor of $\eta < 1$ the magnitude of the solar radiation pressure force (with respect to the ideal case) without altering its direction [12]. The simplified force models are still used in optimization problems for mission applications, in order to reduce their complexity and computational costs [13, 14]. However, as is thoroughly discussed in Ref. [9], when a more realistic reflection model is used [15, 16, 17, 18], as it happens for the optical force model [11], the optimal control law cannot be obtained in a completely analytical form. Even though the approach described in Ref. [9] has been shown, along the years, to be a useful tool for analyzing the optimal performance of a solar sail with an optical force model in various mission scenarios [19], the algorithm proposed in Ref. [9] has some intrinsic limitations. In fact, the determination of the optimal direction of the normal to the sail plane, which must be calculated at each simulation step, requires the use of a root-finding method.

The aim of this work is to start from the exact mathematical model of Ref. [9] and to introduce a suitable approximation to the propulsive acceleration model such that the optimal steering law may be obtained in a completely analytical form. It will be shown that the new solution turns out to be extremely accurate and capable of describing the impact of the thermo-optical characteristics of the sail film on the optimal steering law within a wide range of mission scenarios.

2. Solar sail propulsive acceleration model

The propulsive acceleration $\boldsymbol{a}$ of a flat solar sail, at a distance r from the Sun, can be conveniently described by means of the optical force model [9, 11, 10] as

$$\boldsymbol{a} = \frac{2\,P_{\oplus}\,A_s}{m}\,\left(\frac{r_{\oplus}}{r}\right)^2\,(\hat{\boldsymbol{n}}\cdot\hat{\boldsymbol{r}})\,[b_1\,\hat{\boldsymbol{r}} + (b_2\,\hat{\boldsymbol{n}}\cdot\hat{\boldsymbol{r}} + b_3)\,\hat{\boldsymbol{n}}] \tag{1}$$

where $P_{\oplus} = 4.563\,\mu\mathrm{N/m^2}$ is the solar radiation pressure at a distance $r = r_{\oplus} \triangleq 1\,\mathrm{au}$ from the Sun, A_s is the sail area, m is the solar sail-based spacecraft total mass, $\hat{\boldsymbol{r}}$ is the Sun-sail (radial) unit vector, and $\hat{\boldsymbol{n}}$ is the unit vector normal to the sail plane in the direction opposite to the Sun, see Fig. 1.

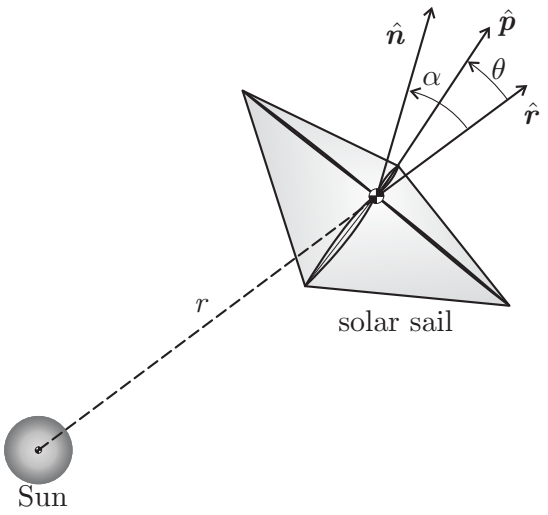

Figure 1: Flat solar sail characteristic angles.

In Eq. (1), b_1, b_2, and b_3 are the force coefficients, defined as

$$b_1 = \frac{1 - \rho\, s}{2} \tag{2}$$

$$b_2 = \rho\, s \tag{3}$$

$$b_3 = \frac{B_f\, \rho\, (1 - s)}{2} + \frac{(1 - \rho)\, (\epsilon_f\, B_f - \epsilon_b\, B_b)}{2\, (\epsilon_f + \epsilon_b)} \tag{4}$$

where ρ is the reflection coefficient, s is the fraction of photons that are specularly reflected, B_f (or B_b) is the non-Lambertian coefficient of the front (or back) sail surface, ϵ_f (or ϵ_b) the emissivity coefficient of the front (or back) sail surface. Note that in the special case $\hat{\boldsymbol{n}} \equiv \hat{\boldsymbol{r}}$ (i.e., for a Sun-facing sail) and $r = r_\oplus$, the modulus of the propulsive acceleration is usually called spacecraft characteristic acceleration and is referred to as a_c. From Eq. (1), it is found that

$$a_c = \frac{2\, P_\oplus\, A_s}{m}\, (b_1 + b_2 + b_3) \tag{5}$$

which represents the standard performance metric in the solar sail field. In particular, the value of a_c depends on the geometrical characteristics of the sail (through the sail surface), the thermo-optical characteristics of the sail film and the spacecraft total mass.

Some special cases can be obtained from Eq. (1). For example, when all of the photons are reflected ($\rho = 1$) with specular reflection ($s = 1$), the force coefficients reduce to $b_1 \equiv b_3 = 0$ and $b_2 = 1$. This model provides the maximum theoretical propulsive acceleration of a solar sail and is usually referred to as "ideal" sail force model. In that case [11], the modulus of the propulsive acceleration at a given distance r from the Sun only depends on the square of the cosine of the cone angle α, defined as the angle between $\hat{\boldsymbol{r}}$ and $\hat{\boldsymbol{n}}$. Another special case is obtained for a perfectly absorbing ($\rho = 0$) and uniform ($\epsilon_f = \epsilon_b$ and $B_f = B_b$) solar sail, whose force coefficients are $b_1 = 1/2$ and $b_2 \equiv b_3 = 0$. In all of the other intermediate cases, characterized by an incomplete reflection and/or a partial re-emission of the impinging photons, what Forward [20] expressively call "grey" solar sails, the force coefficients depend on the physical characteristics of the sail's reflecting film. For example, the force coefficients corresponding to a sail film with a highly reflective aluminum coated front side and a highly emissive chromium-coated backside are given Tab. 1. These data come from a study developed at JPL in 1978 for a rendezvous mission (eventually ruled out) to

model	ρ	s	B_f	B_b	ϵ_f	ϵ_b	b_1	b_2	b_3
ideal	1	1	2/3	2/3	0	0	0	1	0
JPL-1978	0.88	0.94	0.79	0.55	0.05	0.55	0.0864	0.8272	−0.0055
JPL-2015	0.91	0.94	0.79	0.67	0.025	0.27	0.0723	0.8554	−0.0030

Table 1: Optical and force coefficients for a flat solar sail with an ideal [11] and an optical [10, 21] force model.

the Halley's comet using a solar sail as the primary propulsive system [10]. The corresponding mathematical model will now be referred to as JPL-1978 model.

The force coefficients of the JPL-1978 model have been assumed, along the years, as the reference data for the performance estimation of a realistic solar sail. Recently [21], these data have been revised with the aid of new experimental tests conceived in support of NASA's solar sail missions NEA Scout [4] and Lunar Flashlight [5]. The new values of the thermo-optical coefficients of the reflecting film and of the force coefficients are summarized in Tab. 1. A solar sail with these new characteristics will be referred to as JPL-2015 model. Using the data of Tab. 1, the coefficient b_2 for both JPL-1978 and JPL-2015 configurations is about 15% smaller than the same coefficient for an ideal sail. Also, b_1 is about 1/10 of b_2, while b_3 is very small, on the order of a few thousandths. Just this smallness of $|b_3|$ is at the heart of a new analytical solution of the optimal control law that is discussed later on.

Before proceeding on, it is useful to note that the propulsive acceleration vector $\boldsymbol{a}$ can equivalently be decomposed along two orthogonal directions, characterized by unit vectors $\hat{\boldsymbol{n}}$ (normal to the sail) and $\hat{\boldsymbol{t}}$

(parallel to the sail plane). Accordingly, the propulsive acceleration can be written as

$$\boldsymbol{a} = a_{\perp}\,\hat{\boldsymbol{n}} + a_{\parallel}\,\hat{\boldsymbol{t}} \tag{6}$$

where, taking into account Eq. (1), it is found that

$$a_{\perp} = \frac{2\,P_{\oplus}\,A_s}{m}\,\left(\frac{r_{\oplus}}{r}\right)^2\,\left[(b_1+b_2)\,\cos^2\alpha + b_3\,\cos\alpha\right] \tag{7}$$

$$a_{\parallel} = \frac{2\,P_{\oplus}\,A_s}{m}\,\left(\frac{r_{\oplus}}{r}\right)^2\,b_1\,\sin\alpha\,\cos\alpha \tag{8}$$

3. Known results for the optimal steering laws

A classical problem involving the optimal control of a flat solar sail consists of finding the orientation of the normal unit vector $\hat{\boldsymbol{n}}$ (or that of the symmetry axis for an axially symmetric solar sail [22]) which maximizes the projection of the propulsive acceleration $\boldsymbol{a}$ along a given unit vector $\hat{\boldsymbol{q}}$, see Fig. 1. A first example of this kind of problem is obtained when a minimum-time transfer trajectory between two given heliocentric orbits is sought using an indirect approach [7]. In that case the optimal control law is found by maximizing, at any time, the projection of the propulsive acceleration along the direction of the Lawden's primer vector [23]. A second example comes from the problem of increasing the semimajor axis of the solar sail osculating orbit by maximizing the projection of $\hat{\boldsymbol{a}}$ along the direction of the spacecraft inertial velocity [24, 25].

In mathematical terms, for a given unit vector $\hat{\boldsymbol{q}}$, the problem of maximizing the projection of $\boldsymbol{a}$ (given by Eq. (1)) along $\hat{\boldsymbol{q}}$ amounts to finding the unit vector $\hat{\boldsymbol{n}}$ that maximises, at any instant, the scalar performance index J defined as

$$J \triangleq (\hat{\boldsymbol{n}}\cdot\hat{\boldsymbol{r}})\,\left[b_1\,\hat{\boldsymbol{r}}\cdot\hat{\boldsymbol{q}} + (b_2\,\hat{\boldsymbol{n}}\cdot\hat{\boldsymbol{r}} + b_3)\,\hat{\boldsymbol{n}}\cdot\hat{\boldsymbol{q}}\right] \tag{9}$$

In the special case when $\hat{\boldsymbol{q}} \equiv \hat{\boldsymbol{r}}$, J takes its maximum if $\hat{\boldsymbol{n}} = \hat{\boldsymbol{r}}$, that is, for a Sun-facing solar sail. Indeed, in that case Eq. (9) becomes an increasing function of the scalar variable $\hat{\boldsymbol{n}}\cdot\hat{\boldsymbol{r}}$ only. Another particular situation happens when $\hat{\boldsymbol{q}} = -\hat{\boldsymbol{r}}$. Equation (9) states that the maximum value of J is zero, and this is obtained when $\hat{\boldsymbol{n}}$ is orthogonal to the Sun-sail line, i.e. when $\hat{\boldsymbol{n}}\cdot\hat{\boldsymbol{r}} = 0$ and the propulsive thrust vanishes, see Eq. (1).

The general case when $\hat{\boldsymbol{q}}\times\hat{\boldsymbol{r}} \neq 0$ is, instead, more involved. According to Ref. [9], a necessary condition for maximizing J is that $\hat{\boldsymbol{n}}$ belongs to the plane $\mathcal{P}$ spanned by $\hat{\boldsymbol{q}}$ and $\hat{\boldsymbol{r}}$ and may be written as

$$\hat{\boldsymbol{n}} = \frac{\sin(\theta-\alpha)}{\sin\theta}\,\hat{\boldsymbol{r}} + \frac{\sin\alpha}{\sin\theta}\,\hat{\boldsymbol{q}} \tag{10}$$

where the cone angles $\theta \in [0,\,\pi]$, and $\alpha \in [0,\,\pi/2]$ are defined as

$$\alpha \triangleq \arccos\left(\hat{\boldsymbol{n}}\cdot\hat{\boldsymbol{r}}\right) \qquad , \qquad \theta \triangleq \arccos\left(\hat{\boldsymbol{q}}\cdot\hat{\boldsymbol{r}}\right) \tag{11}$$

Note that the limitation $\alpha < \pi/2$ comes from the fact that the propulsive acceleration cannot have a radial component pointing towards the Sun, whereas the direction of $\hat{\boldsymbol{q}}$ (and therefore θ) is free of such a constraint. The problem is now to find the optimal sail cone angle $\alpha = \alpha^{\star}$ that maximizes J. Substituting Eqs. (10)-(11) into (9), the performance index reduces to

$$J = \cos\alpha\,\left[b_1\,\cos\theta + (b_2\,\cos\alpha + b_3)\,\cos\left(\theta-\alpha\right)\right] \tag{12}$$

For a given triplet $\{b_1, b_2, b_3\}$, the optimal cone angle is [9]

$$\alpha^{\star}(\theta) = \begin{cases} \widetilde{\alpha}(\theta) & \text{if} \quad J|_{\alpha=\widetilde{\alpha}(\theta)} > 0 \\ \pi/2 & \text{if} \quad J|_{\alpha=\widetilde{\alpha}(\theta)} \leq 0 \end{cases} \tag{13}$$

where $\widetilde{\alpha}(\theta)$ is the sail cone angle that meets the necessary and sufficient conditions for a local maximum of J, viz.

$$\left.\frac{\partial J}{\partial\alpha}\right|_{\alpha=\widetilde{\alpha}(\theta)} = 0 \qquad \cap \qquad \left.\frac{\partial^2 J}{\partial\alpha^2}\right|_{\alpha=\widetilde{\alpha}(\theta)} < 0 \tag{14}$$

An analytical form of the function $\widetilde{\alpha}(\theta)$ is available for an ideal force model only, see Tab. 1, and the solution was first discover by Sauer in 1976 [7]. It is given by

$$\tan\widetilde{\alpha}(\theta) = \frac{-3\,\cos\theta + \sqrt{8+\cos^2\theta}}{4\,\sin\theta} \qquad \text{if} \qquad b_1 = b_3 = 0 \tag{15}$$

Notably, a simplified version of this solution exists, since, using some trigonometrical identities, it can be verified that

$$\widetilde{\alpha}(\theta) = \frac{\theta - \arcsin\left(\dfrac{\sin\theta}{3}\right)}{2} \qquad \text{if} \qquad b_1 = b_3 = 0 \tag{16}$$

Unfortunately, for the general optical force model, i.e. when $b_1 \neq 0$ and $b_3 \neq 0$, the treatment of Ref. [9] shows than an analytical solution in the form $\widetilde{\alpha} = \widetilde{\alpha}(\theta)$ cannot be obtained from Eqs. (14). Indeed, the solution of Eqs. (14) is

$$\tan\theta = \frac{\sin\widetilde{\alpha}\left(3\,b_2\,\cos^2\widetilde{\alpha} + 2\,b_3\,\cos\widetilde{\alpha} + b_1\right)}{3\,b_2\,\cos^3\widetilde{\alpha} + 2\,b_3\,\cos^2\widetilde{\alpha} - 2\,b_2\,\cos\widetilde{\alpha} - b_3} \tag{17}$$

while the condition $J|_{\alpha=\widetilde{\alpha}(\theta)} > 0$ in Eq. (13) translates into

$$J|_{\alpha=\widetilde{\alpha}(\theta)} > 0 \quad \text{if} \quad \widetilde{\alpha} < \arccos\left(\frac{-b_1\,b_3 - 2\,b_2\,b_3 + \sqrt{b_1^2\,b_3^2 - 4\,b_1\,b_3^2\,b_2 + 8\,b_1^2\,b_2^2 + 4\,b_2^3\,b_1}}{4\,b_1\,b_2 + 2\,b_2^2}\right) \tag{18}$$

which constraints the maximum admissible value of $\widetilde{\alpha}$. For example, for a JPL-1978 model, Eq. (18) provides $\widetilde{\alpha} < 72.6\,\text{deg}$, while for the JPL-2015 case the result is $\widetilde{\alpha} < 74.2\,\text{deg}$, see Tab. 1. In both cases these numbers are well below the maximum admissible value of 90 deg, which can be reached by an ideal solar sail. In fact, in the ideal case, substituting $b_1 = b_3 = 0$ in Eq. (18), it is found that $J|_{\alpha=\widetilde{\alpha}(\theta)} > 0$ when $\alpha < 90\,\text{deg}$, which implies that Eq. (16) is valid for any α within its admissible range of variation.

The algorithm for calculating the optimal steering law, which is thoroughly discussed in Ref. [9], can be summarized as follows. For a given value of θ, the value of $\widetilde{\alpha}$ is first found from Eq. (17) using a numerical approach. The corresponding optimal cone angle $\alpha^\star$ is calculated from Eq. (13) taking into account the constraint of Eq. (18). Finally, the optimal direction of $\hat{\boldsymbol{n}}$ is obtained from Eq. (10) with the substitution $\alpha = \alpha^\star$. As stated, such a procedure requires the numerical solution of a root-finding problem for each value of θ, and can therefore become computationally expensive when the optimal thrust direction must be calculated many times. This happens, for example, when the optimal trajectory of a low-performance solar sail is sought, since the computation of $\hat{\boldsymbol{n}}$ must be repeated for each integration step of the equations of motion. A possible simplification of the procedure can be obtained when the thermo-optical characteristics of the sail are given, that is, when the triplet $\{b_1, b_2, b_3\}$ is fixed. In that case the function $\widetilde{\alpha} = \widetilde{\alpha}(\theta)$ can be obtained by interpolation from Eq. (17), but this approach introduces some unavoidable errors in the evaluation of $\hat{\boldsymbol{n}}$. Also, it is not very flexible, as the interpolating function must be changed whenever a force coefficient is changed. This may occur, for example, due to a variation of the reflecting film material [26], or to the availability of new experimental measurements [21], or even to the sail degradation effects during the mission [27, 28].

For these reasons the next section describes a new approach that allows the optimal sail cone angle to be calculated in an analytical form. This result is based on a suitable simplification of the functional J that has only a very minor effect on the estimate of the optimal direction of $\hat{\boldsymbol{n}}$.

4. Analytical solution of the optimal steering law

As stated in the previous section, an analytical solution of the optimal steering law for a solar sail is possible only in the case of an ideal force model. In the general case when the three force coefficients b_1, b_2 and b_3 are all different from zero, the obstacle against an analytic version of the optimal steering law is represented by the difficulty of inverting Eq. (17) in the form $\widetilde{\alpha} = \widetilde{\alpha}(\theta)$. However, it will now be shown that this problem becomes analytically solvable provided a suitable approximation is introduced in the mathematical (force) model. Such an approximation is based on the fact that the reflecting film of a conventional solar sail is designed such to draw the sail performance up to that of an ideal (perfectly

reflecting) solar sail. Clearly, this remark does not apply to solar sails whose surface contains electrochromic material [29, 30] with optical properties that can be varied on application of a voltage. The use of those materials is useful for different applications, including the possibility of varying the modulus of the propulsive thrust without changing the solar sail attitude [31, 32, 33], or that of generating suitable torques for attitude control, as recently shown by the Japanese solar sail demonstrator IKAROS [34, 35, 36].

Returning to a conventional solar sail, its performance approaches that of an ideal sail provided the force coefficient b_2 is much greater than b_1 and b_3 (recall that for an ideal sail b_2 is the only coefficient different from zero). This is confirmed by the data reported in Tab. 1 where in both cases involving the JPL sail the ratio b_1/b_2 is about 0.1, while the ratio $|b_3/b_2|$ is a few thousandths only. This last remark is now used for a suitable simplification of the sail force model. To this end, note that Eq. (1) can be equivalently rewritten in terms of a component a_r along the radial direction $\hat{\boldsymbol{r}}$, and a component a_n along the normal $\hat{\boldsymbol{n}}$ to the sail nominal plane, that is, $\boldsymbol{a} = a_r\hat{\boldsymbol{r}} + a_n\hat{\boldsymbol{n}}$, with

$$a_n = \frac{2\,P_\oplus\,A_s}{m}\,\left(\frac{r_\oplus}{r}\right)^2\,f\,\cos\alpha \tag{19}$$

where f is an auxiliary function defined by

$$f \triangleq b_2\,\cos\alpha + b_3 \tag{20}$$

Assuming that the cone angle is not close to its maximum value of 90 deg, an excellent approximation of f can be easily found. Recalling that $|b_3/b_2|$ is very small, one would be tempted to simply neglect b_3 compared to b_2 and set

$$f \simeq f_0 \triangleq b_2\,\cos\alpha \tag{21}$$

However, a better approximation exists. This is given by

$$f \simeq f_a \triangleq (b_2 + b_3)\,\cos\alpha \tag{22}$$

which is obtained by formally replacing b_3 with $b_3\,\cos\alpha$ in Eq. (20). The superiority of the approximation f_a with respect to f_0 can be verified by introducing the relative error, defined as

$$\varepsilon \triangleq \left|\frac{a_n^{(a)} - a_n}{a_n}\right| \tag{23}$$

where $a_n^{(a)}$ is the approximate form of a_n, obtained by substituting either f_0 or f_a in place of f into Eq. (19).

A comparison between the errors induced by approximations of Eqs. (21) and (22) is shown in Fig. 2, where the value of b_3 in Eq. (22) is -0.0030, equal to that corresponding to a JPL-2015 model, see Tab. 1. Clearly, the approximation with f_a is better than that with f_0 for all cone angles. Replacing therefore f with f_a in Eq. (19), and noting that

$$\varepsilon \equiv \left|\frac{f_a - f}{f}\right| = \left|\frac{(b_3/b_2)\;(\cos\alpha - 1)}{(b_3/b_2) + \cos\alpha}\right| \tag{24}$$

the impact of the relative error on the obtainable results can be parameterized as a function of the ratio b_3/b_2, see Fig. 3(a). The figure shows that as long as $|b_3/b_2| < 0.01$ and $\alpha < 80\,\text{deg}$, the relative error ε is less than 5%. Assuming, for example, $\alpha \leq 75\,\text{deg}$, for a JPL-1978 model the error is less than 2%, while for the JPL-2015 case it is below 1%, see Fig. 3(b). Finally note that the approximation (20) does not affect the component a_r along the radial direction $\hat{\boldsymbol{r}}$, which indeed remains unchanged.

There is an interesting, physical, interpretation of the approximation $f \simeq f_a$ that deserves some comments. In fact, when b_3 is replaced with $b_3\,\cos\alpha$ as per Eq. (20), the component of the propulsive acceleration normal to the sail plane, see Eq. (7), becomes

$$a_\perp = \frac{2\,P_\oplus\,A_s}{m}\,\left(\frac{r_\oplus}{r}\right)^2\,\eta\,\cos^2\alpha \tag{25}$$

where

$$\eta \triangleq b_1 + b_2 + b_3 \tag{26}$$

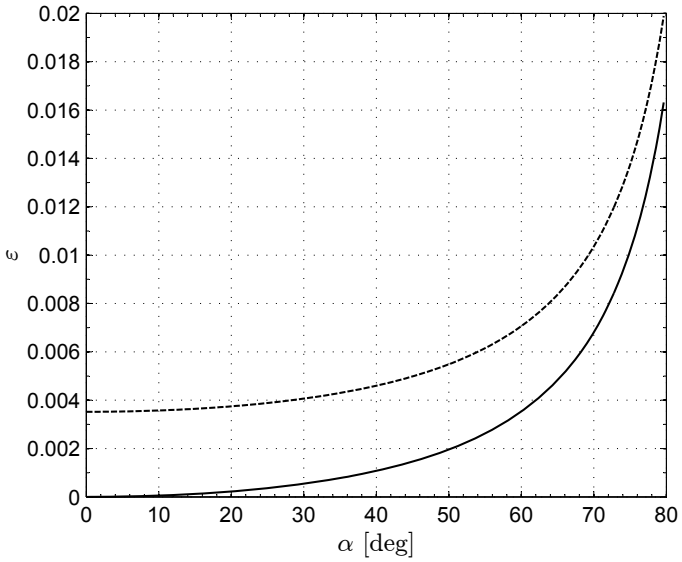

Figure 2: Relative error ε obtained with approximation f_0 (dotted line) and f_a with $b_3 = -0.0030$ (solid line) as a function of cone angle α.

Notably, Eq. (25) coincides with the sail acceleration of the so called η-perfect reflection (η-PR) model [12]. The new approximate model, which will be referred to as η-optical reflection (η-OR) model, is therefore mathematically described by Eq. (6), where $a_\perp$ is given by Eq. (25) and $a_\parallel$ is obtained from Eq. (8). The η-OR model represents an improvement of the η-PR model, which does not account for the sail acceleration component parallel to the sail plane, and is nearly coincident with the optical force model, the only (minor) difference between the two models being in the $\cos\alpha$ that multiplies b_3 in the $a_\perp$ component. The advantage of the η-OR is that, unlike the classical optical force model, the former allows an analytical solution of the optimal control law to be found, as is now shown.

4.1. Optimal cone angle

When Eq. (22) is substituted into Eq. (12), the functional to be maximized takes the following new expression

$$\frac{J}{b_2 + b_3} \simeq J_a \triangleq \cos\alpha \, [B \, \cos\theta + \cos\alpha \, \cos(\theta - \alpha)] \tag{27}$$

where

$$B \triangleq \frac{b_1}{b_2 + b_3} \tag{28}$$

is a sort of reduced force coefficient that relates the approximate functional J_a with the thermo-optical characteristics of the reflecting film. In the spirit of approximation (22), and observing that $b_2 + b_3 > 0$, the cone angle $\alpha_a^\star$ that maximizes J_a turns out to be an estimate of the optimal cone angle $\alpha^\star$ that maximizes J.

From a mathematical viewpoint, for a given value of B, the function $\alpha_a^\star = \alpha_a^\star(\theta)$ must meet the same conditions given by Eqs. (13)-(14) when J is formally substituted with J_a, $\alpha^\star$ with $\alpha_a^\star$, and $\widetilde{\alpha}$ with $\widetilde{\alpha}_a$, where $\widetilde{\alpha}_a = \widetilde{\alpha}_a(\theta)$ is the solution of the necessary condition $\partial J_a / \partial \alpha = 0$. The advantage of using J_a instead of J is that it is possible to obtain a simple analytic expression of $\widetilde{\alpha}_a$ as a function of θ. To prove this claim, first note that $\cos\alpha \geq 0$ within the range of variation of the cone angle. Therefore, J_a satisfies the following relation

$$J_a(\alpha) > 0 \qquad \text{when} \qquad \tan\theta < -\frac{\cos^2\alpha + B}{\cos\alpha \, \sin\alpha} \tag{29}$$

with

$$\frac{\partial J_a}{\partial \alpha} = 3 \, \sin\theta \, \cos^3\alpha - 3 \, \cos\theta \, \sin\alpha \, \cos^2\alpha - 2 \, \sin\theta \, \cos\alpha - B \, \cos\theta \, \sin\alpha \tag{30}$$

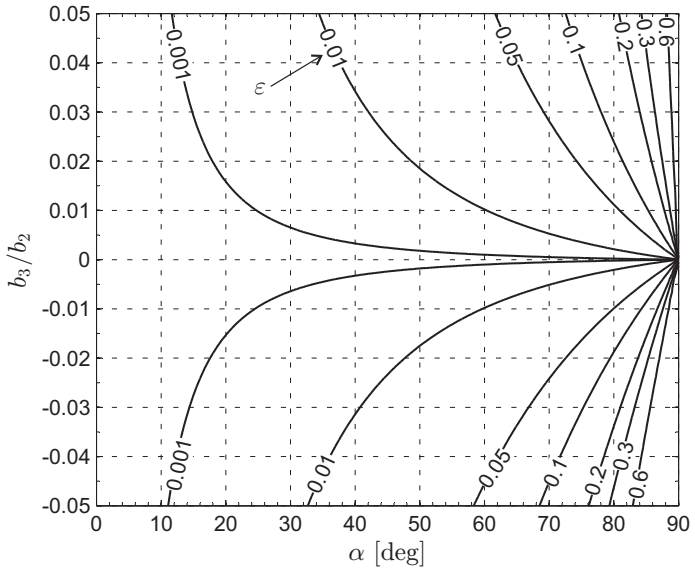

(a) Level curve of ε, see Eq. (24).

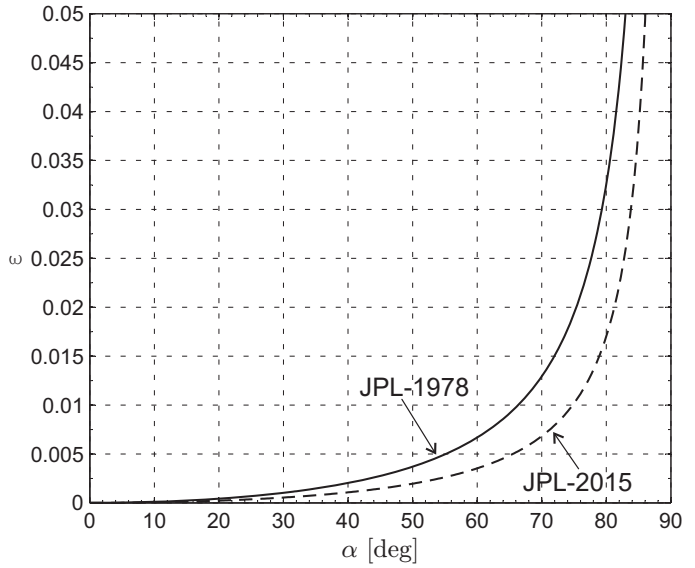

(b) Case of JPL-1978 and JPL-2015.

Figure 3: Relative error ε as a function of cone angle α and the ratio b_3/b_2.

In the special case of $\theta = \pi/2$, the previous equation states that $\partial J_a/\partial\alpha = 0$ if $\alpha = \arccos\sqrt{2/3}$.

Recalling that $\alpha \in [0, \pi/2]$, and using the substitution

$$\alpha \triangleq \arctan x \qquad \text{with} \qquad x \geq 0 \tag{31}$$

Eqs. (29) and (30) can be rewritten in terms of the new auxiliary variable x as

$$J_a(x) > 0 \qquad \text{when} \qquad \tan\theta < -B\,x - \frac{B+1}{x} \tag{32}$$

and

$$\frac{\partial J_a}{\partial \alpha} = -\frac{\cos\theta\,\left[B\,x^3 + 2\,\tan\theta\,x^2 + (B+3)\,x - \tan\theta\right]}{\sqrt{(x^2+1)^3}} \quad \text{with} \quad \theta \neq \pi/2 \tag{33}$$

respectively. From the last relation, the necessary condition $\partial J_a/\partial\alpha = 0$ amounts to looking for the positive real roots of the following third order polynomial

$$Q(x) \triangleq B\,x^3 + 2\,\tan\theta\,x^2 + (B+3)\,x - \tan\theta \quad \text{with} \quad \theta \neq \pi/2 \tag{34}$$

In general, the three roots x_1, x_2, and x_3 of $Q(x)$ can be found analytically [37] as a function of $\tan\theta$ (recall that $\theta \neq \pi/2$) and of the reduced force coefficient B as

$$x_1 = A\,\cos\left(\frac{\phi}{3}\right) + D \tag{35}$$

$$x_2 = A\,\cos\left(\frac{\phi + 2\,\pi}{3}\right) + D \tag{36}$$

$$x_3 = A\,\cos\left(\frac{\phi + 4\,\pi}{3}\right) + D \tag{37}$$

where

$$A \triangleq 2\sqrt{\frac{4\,\tan^2\theta}{9\,B^2} - \frac{1}{B} - \frac{1}{3}} \tag{38}$$

$$\phi \triangleq \arccos\left[\frac{\tan\theta\,\left(45\,B^2 + 54\,B - 16\,\tan^2\theta\right)}{2\sqrt{\left(4\,\tan^2\theta - 9\,B - 3\,B^2\right)^3}}\right] \tag{39}$$

$$D \triangleq -\frac{2\,\tan\theta}{3\,B} \tag{40}$$

To simplify the discussion, it is useful to introduce the following notations related to Eqs. (38) and (39)

$$\theta_1 \triangleq \arctan\left[\frac{\sqrt{3\,B\,(B+3)}}{2}\right] \tag{41}$$

$$\theta_2 \triangleq \arctan\left[\frac{\sqrt{84\,B + \sqrt{3\,(B+2)\,(11\,B+6)^3} + 59\,B^2 - 36}}{8}\right] \tag{42}$$

$$\theta_3 \triangleq \pi - \theta_2 \tag{43}$$

It can be verified that: a) if $\theta > \theta_3$, no positive real root exists for $Q(x)$; b) if $\pi/2 < \theta \leq \theta_3$, there are two positive real roots, x_1 and x_3, with $x_3 \leq x_1$; c) if $\theta_1 < \theta < \pi/2$, the only positive real root is x_1; d) if $\theta \leq \theta_1$, the only positive real root is x_3.

With reference to the roots of Eq. (34), the existence of either three real roots, or a single real root and two complex conjugate roots, depends on the value of A and ϕ in Eqs. (38)-(39). In fact, $A \in \mathbb{R}$ if the argument of the square root in Eq. (38) is nonnegative, while $\phi \in \mathbb{R}$ if the argument of the inverse cosine is real and less than one. Also note that the inequality $\tan\theta < -B\,x - (B+1)/x$ of Eq. (32) can be rewritten as a function of x only, by calculating $Q(x) = 0$ through Eq. (34) and solving for $\tan\theta$. The result is

$$\frac{B\,x^3 + (B+3)\,x}{1 - 2\,x^2} < -B\,x - \frac{B+1}{x} \tag{44}$$

The equivalent version of Eq. (32) is therefore

$$J_a(x) > 0 \quad \cap \quad Q(x) = 0 \qquad \text{if} \qquad x < \frac{\sqrt{B^2 + B}}{B} \tag{45}$$

This last result can be conveniently translated into a relation that involves θ, that is

$$J_a(x) > 0 \quad \cap \quad Q(x) = 0 \qquad \text{if} \qquad \theta < \theta_4 \tag{46}$$

where

$$\theta_4 \triangleq \pi - \arctan\left[2\sqrt{B^2 + B}\right] \tag{47}$$

In other terms, Eq. (46) states that when $\theta < \theta_4$, the positive real roots of $Q(x) = 0$ provide a positive value of J_a.

Observing that $\pi/2 < \theta_4 \leq \theta_3$, and bearing in mind Eq. (31), the following analytical solution for the cone angle $\alpha_a^\star$ that maximizes J_a is eventually obtained

$$\alpha_a^\star(\theta) = \begin{cases} \arctan(x_3) & \text{if} \quad \theta \leq \theta_1 \\ \arctan(x_1) & \text{if} \quad \theta_1 < \theta < \pi/2 \\ \arccos\sqrt{2/3} & \text{if} \quad \theta = \pi/2 \\ \arctan(x_3) & \text{if} \quad \pi/2 < \theta \leq \theta_4 \\ \pi/2 & \text{if} \quad \theta_4 < \theta \leq \pi \end{cases} \tag{48}$$

where x_1 and x_3 are given by Eqs. (35) and (37) as a function of $\{\tan\theta, B\}$, whereas θ_1 and θ_4 are given by Eqs. (41) and (47) as a function of B only. Note that in the ideal case when $B = 0$ the condition about the sign of J_a, given by Eq. (32), is automatically satisfied, since x is positive. Also, when $B = 0$ the order of polynomial $Q(x)$ reduces to two, see Eq. (34). In fact, in the ideal force model case, the only positive real root of $Q(x)$, corresponding to a local maximum of J_a, is

$$x = \frac{-3 + \sqrt{9 + 8\,\tan^2\theta}}{4\,\tan\theta} \tag{49}$$

which, taking into account Eq. (31), coincides with the classical result of Eq. (15).

5. Validation of the analytical results

The effectiveness of the analytical steering law discussed in the previous section is now checked by comparing the values of $\alpha_a^\star$ given by Eq. (48) with those obtained using the approach described in Ref. [9], which requires the use of a numerical method for the solution of the necessary condition (14). For the sake of example, we use the force coefficients of JPL-1978 and JPL-2015 cases reported in Tab. 1. The corresponding values of the reduced force coefficients are $B = 0.10514$ for the JPL-1978 model and $B = 0.084819$ for the JPL-2015 case. Figs. 4(a)-4(b) show the variation of the optimal cone angle as a function of θ.

The figures demonstrate that the proposed analytical model is able to accurately approximate the exact results obtained using the approach of Ref. [9]. In particular, the maximum absolute difference in terms of cone angle between the two models, for a given θ, is on the order of a few tenth degree only for both example sails. The analytical model is also able to accurately predict the condition at which the optimal cone angle takes the value of 90 deg. In fact, from Eq. (46), the discontinuity in the function $\alpha^\star = \alpha^\star(\theta)$ is obtained at $\alpha^\star > 72.86\,\text{deg}$ for a JPL-1978 model and at $\alpha^\star > 74.38\,\text{deg}$ for the case of JPL-2015 model. Notably, Fig. 4(b) illustrates, for the first time, the optimal control law for a flat solar sail with the optical force model that takes into account the new force coefficients obtained by the recent experimental analyses discussed by Heaton and Artusio-Glimpse [21].

The analytical control law has been further validated by simulating an optimal, heliocentric, orbital transfer. In particular, the optimal control law developed in this paper has been applied to a two-dimensional circular orbit-to-orbit Earth-Mars transfer using solar sails with optical force coefficients equal to the case of JPL-1978 model with various values of characteristic accelerations. For all of the simulated transfers, a direct interplanetary insertion of the solar sail at Earth with zero hyperbolic excess energy has been assumed. Accordingly, the initial Sun-spacecraft distance is $r_0 = r_\oplus$, whereas the spacecraft inertial velocity coincides with the local circular velocity $\sqrt{\mu_\odot/r_\oplus}$, where $\mu_\odot$ is the Sun's gravitational parameter. Note that the

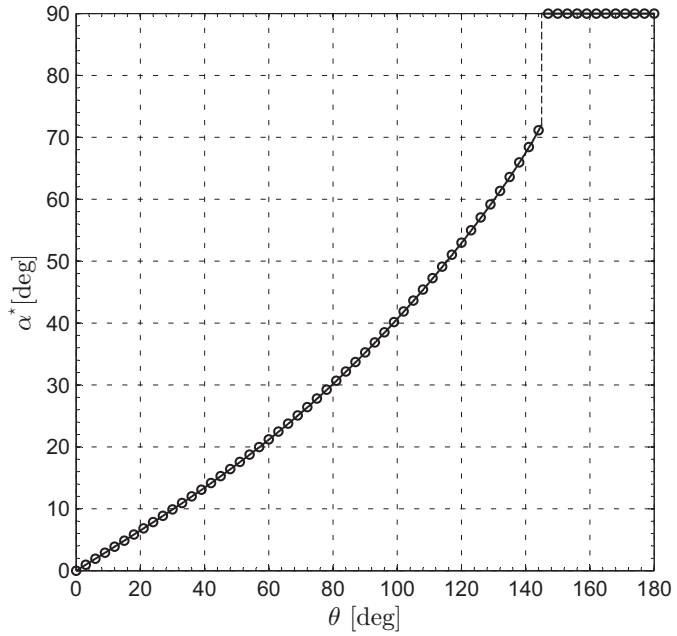

(a) case of JPL-1978.

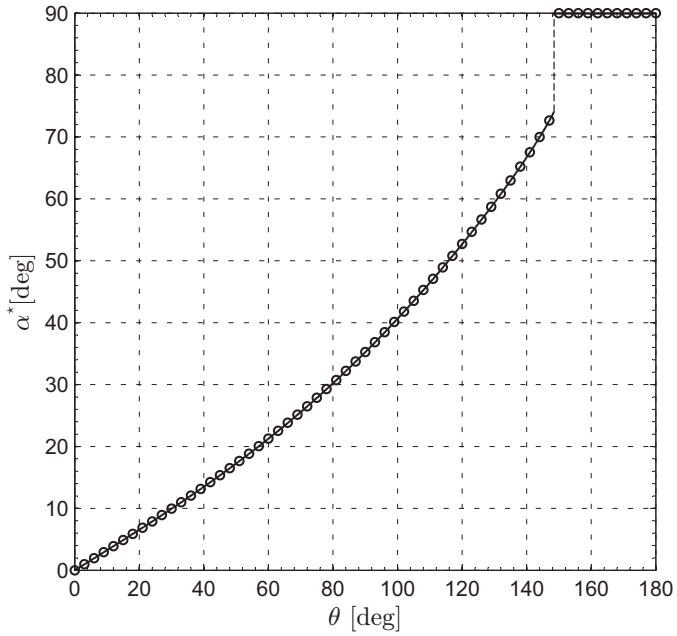

(b) Case of JPL-2015.

Figure 4: Optimal cone angle $\alpha^{\star}$ as a function of θ evaluated through the exact method of Ref. [9] (solid line) and the analytical approximate method (circle).

optimal transfer trajectory is simulated in an ephemeris-free model, i.e. by neglecting the actual position of the two planets in their heliocentric orbits. The minimum times are shown in Fig. 5 by comparing the results attainable with the exact procedure of Ref. [9] and those calculated with the new analytical control law. The transfer times are nearly coincident, with maximum absolute differences (for a given value of a_c) that do not exceed a few hours when the total mission time is on the order of several hundreds days. In this sense, the error is always less than 0.1%.

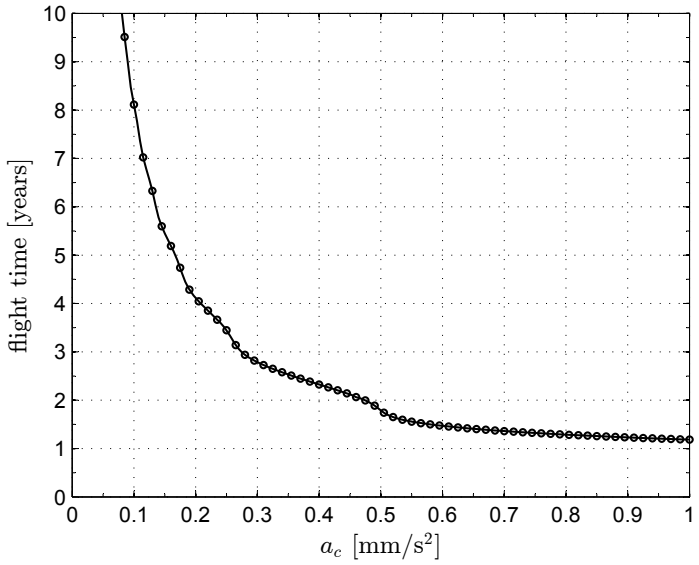

Figure 5: Earth-Mars minimum-time transfers calculated with the exact method (solid line) and the analytical approximate method (circle) for a JPL-1978 model.

6. Conclusions

A fully analytical solution of the optimal steering law for a flat solar sail has been discussed. The result is based on the introduction of the so called η-OR model, in which the sail propulsive acceleration vector is described by means of a component normal to the sail nominal plane, whose modulus coincides with that of the η-PR model, and a component parallel to sail nominal plane, equal to that provided by an optical force model. As a result, the η-OR model is shown to be an accurate approximation of the classical optical force model.

The effectiveness of the analytical solution of the optimal steering law has been validated by direct comparison with numerical data taken from the literature. The simulation results show that the minimum transfer times calculated with the analytical steering law are nearly exact, with errors on the order of a few hours only for missions of several hundred days.

The new method guarantees a substantial reduction of the complexity of the solar sail optimal control problem, and is particularly useful when a variation of optical coefficients of the solar sail must be taken into account during the preliminary mission design. The algorithm for calculating the optimal direction of the propulsive acceleration is simple to be implemented within numerical routines and may be effectively used to solve trajectory optimization problems with either global or local optimization methods.

Conflict of interest statement

The authors declared that they have no conflicts of interest to this work.

References

[1] Y. Tsuda, O. Mori, R. Funase, H. Sawada, T. Yamamoto, S. Takanao, T. Endo, K. Yonekura, H. Hoshino, J. Kawaguchi, Achievement of IKAROS - japanese deep space solar sail demonstration mission, in: 7th IAA Symposium on Realistic Advanced Scientific Space, Vol. 82, Aosta (Italy), 2011, pp. 183–188.

[2] O. Mori, Y. Tsuda, Y. Shirasawa, T. Saiki, Y. Mimasu, J. Kawaguchi, Attitude control of IKAROS solar sail spacecraft and its flight results, in: 61st International Astronautical Congress, Prague, Czech Republic, 2010, paper IAC-10.C1.4.3.

[3] R. Funase, Y. Shirasawa, Y. Mimasu, O. Mori, Y. Tsuda, T. Saiki, J. Kawaguchi, Fuel-free and oscillation-free attitude control of IKAROS solar sail spacecraft using reflectivity control device, in: 28th International Symposium on Space Technology and Science, Okinawa, Japan, 2011.

[4] L. McNutt, L. Johnson, P. Kahn, J. Castillo-Rogez, A. Frick, Near-earth asteroid (NEA) scout, in: AIAA SPACE 2014 Conference and Exposition, San Diego (CA), 2014, paper AIAA 2014-4435.
[5] P. O. Hayne, B. T. Greenhagen, D. A. Paige, et al., Lunar flashlight: Illuminating the lunar south pole, in: 47th Lunar and Planetary Science Conference, The Woodlands (TX), 2016, paper 2761.
[6] A. N. Zhukov, V. N. Lebedev, Variational problem of transfer between heliocentric orbits by means of solar sail, Cosmic Research 2 (1) (1964) 41–44 .
[7] J. Sauer, C. G., Optimum solar-sail interplanetary trajectories, in: AIAA/AAS Astrodynamics Conference, San Diego (CA), 1976, paper AIAA-76-792.
[8] T. Cichan, R. G. Melton, Optimal trajectories for non-ideal solar sails, Advances in the Astronautical Sciences 109 (3) (2001) 2381–2391 .
[9] G. Mengali, A. A. Quarta, Optimal three-dimensional interplanetary rendezvous using non-ideal solar sail, Journal of Guidance, Control, and Dynamics 28 (1) (2005) 173–177, doi: 10.2514/1.8325.
[10] J. L. Wright, Space Sailing, Gordon and Breach Science Publishers, 1992, pp. 223–233.
[11] C. R. McInnes, Solar Sailing: Technology, Dynamics and Mission Applications, Springer-Praxis Series in Space Science and Technology, Springer-Verlag, Berlin, 1999, pp. 47–53 and 173–180, ISBN: 978-3-540-21062-7.
[12] B. Dachwald, Minimum transfer times for nonperfectly reflecting solar sailcraft, Journal of Spacecraft and Rockets 41 (4) (2004) 693–695, doi: 10.2514/1.6279.
[13] I. Mainenti-Lopes, L. C. Gadelha Souza, F. L. De Sousa, A comparative study between control strategies for a solar sailcraft in Earth-Mars transfer, Mechanical Systems and Signal Processing 79 (2016) 289–296, doi: 10.1016/j.ymssp.2016.02.026.
[14] Y. Gao, J. Wu, The optimal control law for the tethered system formed by an asteroid and a solar sail, Advances in Space Research 57 (4) (2016) 1002–1014, doi: 10.1016/j.asr.2015.12.018.
[15] G. Ono, Y. Tsuda, K. Akatsuka, T. Saiki, Y. Mimasu, N. Ogawa, F. Terui, Generalized attitude model for momentum-biased solar sail spacecraft, Journal of Guidance, Control, and Dynamics 39 (7) (2016) 1491–1500 .
[16] B. A. Campbell, S. J. Thomas, Realistic solar sail thrust, in: M. Macdonald (Ed.), Advances in Solar Sailing, Springer Praxis Books, Springer Berlin Heidelberg, 2014, pp. 407–435.
[17] X. Zeng, F. Jiang, J. Li, Asteroid body-fixed hovering using nonideal solar sails, Research in Astronomy and Astrophysics 15 (4) (2015) 597–607, doi: 10.1088/1674-4527/15/4/011.
[18] J. Simo, C. R. McInnes, Potential effects of a realistic solar sail and comparison to an ideal sail, in: 26th AAS/AIAA Space Flight Mechanics Meeting, 2016, pp. 3106–3120.
[19] J. Heiligers, G. Mingotti, C. R. McInnes, Optimal solar sail transfers between halo orbits of different sun-planet systems, Advances in Space Research 55 (5) (2015) 1405–1421, doi: 10.1016/j.asr.2014.11.033.
[20] R. L. Forward, Grey solar sails, Journal of the Astronautical Sciences 38 (2) (1990) 161–185 .
[21] A. F. Heaton, A. B. Artusio-Glimpse, An update to NASA reference solar sail thrust model, in: AIAA SPACE 2015 Conference and Exposition, Pasadena (CA), 2015, paper AIAA 2015-4506.
[22] G. Mengali, A. A. Quarta, Optimal control laws for axially symmetric solar sails, Journal of Spacecraft and Rockets 42 (6) (2005) 1130–1133, doi: 10.2514/1.17102.
[23] D. F. Lawden, Optimal Trajectories for Space Navigation, Butterworths & Co., London, 1963, pp. 54–60.
[24] M. Macdonald, B. Dachwald, Heliocentric solar sail orbit transfers with locally optimal control laws, Journal of Spacecraft and Rockets 44 (1) (2007) 273–276, doi: 10.2514/1.17297.
[25] G. Mengali, A. A. Quarta, Near-optimal solar-sail orbit-raising from low earth orbit, Journal of Spacecraft and Rockets 42 (5) (2005) 954–958, doi: 10.2514/1.14184.
[26] G. Mengali, A. A. Quarta, C. Circi, B. Dachwald, Refined solar sail force model with mission application, Journal of Guidance, Control, and Dynamics 30 (2) (2007) 512–520, doi: 10.2514/1.24779.
[27] B. Dachwald, G. Mengali, A. A. Quarta, M. Macdonald, Parametric model and optimal control of solar sails with optical degradation, Journal of Guidance, Control, and Dynamics 29 (5) (2006) 1170–1178, doi: 10.2514/1.20313.
[28] B. Dachwald, M. Macdonald, C. R. McInnes, G. Mengali, A. A. Quarta, Impact of optical degradation on solar sail mission performance, Journal of Spacecraft and Rockets 44 (4) (2007) 740–749, doi: 10.2514/1.21432.
[29] C. G. Granqvist, E. Avendano, A. Azens, Electrochromic coatings and devices: survey of some recent advances, Thin Solid Films 442 (1-2) (2003) 201–211, doi: 10.1016/S0040-6090(03)00983-0.
[30] N. Kislov, Variable reflectance/transmittance coatings for solar sail altitude control and three axis stabilization, AIP Conference Proceedings 699 (1) (2004) 103–111, doi: 10.1063/1.1649563.
[31] C. Colombo, C. R. McInnes, Orbital dynamics of "smart-dust" devices with solar radiation pressure and drag, Journal of Guidance, Control and Dynamics 34 (6) (2011) 1613–1631, doi: 10.2514/1.52140.
[32] G. Aliasi, G. Mengali, A. A. Quarta, Artificial lagrange points for solar sail with electrochromic material panels, Journal of Guidance, Control, and Dynamics 36 (5) (2013) 1544–1550, doi: 10.2514/1.58167.
[33] G. Mengali, A. A. Quarta, Heliocentric trajectory analysis of sun-pointing smart dust with electrochromic control, Advances in Space Research 57 (4) (2016) 991–1001, doi: 10.1016/j.asr.2015.12.017.
[34] T. Hu, S. Gong, J. Mu, J. Li, T. Wang, W. Qian, Switch programming of reflectivity control devices for the coupled dynamics of a solar sail, Advances in Space Research 57 (5) (2016) 1147–1158, doi: 10.1016/j.asr.2015.12.029.
[35] J. Van Der Ha, Y. Mimasu, Y. Tsuda, O. Mori, R. Sedwick, Solar and thermal radiation models and flight evaluation for IKAROS solar sail, Journal of Spacecraft and Rockets 52 (3) (2015) 958–967, doi: 10.2514/1.A33158.
[36] T. Yamaguchi, Y. Mimasu, Y. Tsuda, M. Yoshikawa, Hybrid estimation of solar radiation pressure for a spinning solar sail spacecraft, Journal of Spacecraft and Rockets 51 (1) (2014) 381–384, doi: 10.2514/1.A32387.
[37] G. Woan, The Cambridge Handbook of Physics Formulas, Cambridge University Press, 2000, p. 51, ISBN: 978-0-521-57507-2.